Impact Factor (SJIF): 3.632

International Journal of Advance Research in Engineering, Science & Technology

e-ISSN: 2393-9877, p-ISSN: 2394-2444

Volume 3, Issue 7, July-2016

Effects of Silver doping in Hydroxyapatite and its coatings on 316L Stainless Steel.

Ishan Garg, Dr. Uma Batra

([1,2]Materials and Metallurgical Engineering Department, PEC University of Technology)

Abstract- *In this work, hydroxyapatite (HA) and silver doped hydroxyapatite nanopowder (Ag2HA and Ag4HA) were synthesized by the sol-gel method using precursors like calcium nitrate tetra-hydrate (CNT) for calcium, tri-ethyl phosphate (TEP) for phosphorous and silver nitrate (AgNT) for silver and their coatings were deposited using spin coating technique on 316L stainless steel (SS). Then the powders and coated samples were calcined and sintered at 400^{o}C respectively. The Ca/P ratio of the synthesized HA, Ag2HA and Ag4HA nanoparticles were maintained in the range of 1.58–1.70. Various characterization techniques were used to study the compositional structure, functionality and phase changes of powders and microstructure of coatings by using XRF, FTIR, XRD and FE-SEM respectively. The mechanical properties of coatings like micro hardness, surface roughness and adhesion strength were also characterized. Potentiodynamic linear polarization was also done to study the corrosion behavior of coated samples. XRF confirms that silver has been doped successfully and HA, Ag2HA and Ag4HA coatings were successfully and uniformly deposited on 316L SS. Ag4HA showed the good mechanical behavior like its micro hardness and adhesion strength was high and low surface roughness. Corrosion study reveals that Ag4HA has good corrosion resistance.*

Keywords: *Hydroxyapatite, Silver, Sintering, Calcination, Aging.*

I. INTRODUCTION

About 50 million road accidents take place every year, resulting mostly in injuries related to fractures. Since, most of these accidents occur in remote areas, the wounds are left open and exposed to an extended period of time making them prone to infections. With an improved medical facility, in the advance ages of today's world, fractures can be easily treated with bone implantations.

For bone implants and medical purposes, a wide variety of materials are used. These materials include metallic, ceramic, glasses and polymeric biomaterials. In metallic 316L Stainless Steel is widely used for biomedical purposes as fracture repair and joint replacement due to its low cost, strength and excellent biocompatibility [1]. Even 316 L SS are not bioactive and they cannot be directly used because it is more susceptible to corrosion due to the release of Ni^{2+} and Cr^{2+} ions [2] and the release of these ions can cause serious health risks. So, earlier research has shown that these problems can be overcome by depositing the layer of biomaterial called hydroxyapatite, which is the calcium phosphate ceramic $[Ca_{10}(PO4)_{6.}(OH)_2]$. HA is widely used in orthopedic and reconstructive surgery due to its excellent bioactivity and biocompatibility with the human body [3]. HA has a composition which is similar to the mineral composition of the bone. Bioactive HA coating on 316L SS implants is able to stimulate the bone growth and affixation to the implant surface during the early stage of implantation [4]. Even though hydroxyapatite has an excellent biocompatibility, but the problem is that it has slow rate of osteo-integration with bone tissues, less corrosion resistance, poor mechanical properties and less anti microbial effects and hence, limits its applications. So this is the reason, Ca^{2+} and OH^{-} ions are substituted by cations like Zn^{2+}, Mg^{2+}, Zr^{2+}, Ag^{2+} etc. and anions like Cl^{-}, F^{-} etc respectively to enhance their properties like biocompatibility and affects its physical and chemical properties such as crystallinity, thermal stability.

Implantation in the body is always associated with a risk of microbial infection which is more severe in open-fractured bones. Due to which Silver is used as a dopant in HA because it has been used as an antimicrobial agent for centuries. For example, silver vessels used to preserve water and wine during long voyages [5]. Silver incorporated with bioglass displayed significant biological and antibacterial properties. Bir et al. studied the electrochemical deposition of fluorohydroxyapatite doped with Cu^{2+}, Zn^{2+} and Ag^{+} on 316L stainless steel substrates, where the results exhibited an excellent antibacterial activity [6].

In this study, Silver-doped Hydroxyapatite coatings were developed on 316L Stainless Steel using Spin Coating technique. The coatings were characterized in terms of phase and elemental composition, functionality, microstructure study and mechanical stability etc.

All Rights Reserved, @IJAREST-2016

II. MATERIALS AND METHODS

2.1 Preparation of 316L SS specimens

316L SS composition is shown in Table 1. 316L SS samples were cut into 20mm × 20mm size from 316L SS sheet. The burr was removed by grinding the surface. The samples were polished by emery papers which are in sequence 120, 220, 320, 400, 600,800 and 1000 grit to get flat and scratch free surface and then the samples were polished with Aluminum oxide 500µm mesh size. After polishing 316L SS were degreased, washed with distilled water and were placed in ultrasonic bath and then rinsed in acetone before coating.

Table 1: *Chemical composition (wt.%) of AISI 316 L stainless steel.*

Element	C	Mn	P	Si	Cr	Ni	Mo	N	Cu	Fe
Composition	0.3	2	0.025	0.75	16.9	11.2	2.1	0.06	0.03	Balance

2.2 Synthesis using sol-gel process

Hydroxyapatite synthesises was done using sol-gel route by using the precursors like CNT and AgNT which were purchased from Merck and TEP was purchased from Sigma Aldrich.

For HA, Ca/P ratio was maintained at 1.67 and for Ag2HA and Ag4HA, (Ca+Ag)/P ratio was also maintained at 1.67. To prepare HA nanopowder, 1M solution of CNT was prepared by dissolving CNT in ethanol and 0.6M solution of TEP was prepared by dissolving TEP in ethanol separately. Then, the precursors were hydrolyzed by stirring at 700 rpm for 30 min at 27^{o}C. Then 1M CNT solution was added drop wise (4 ml/min) to the 0.6M TEP solution and during addition solution was stirred vigorously at 1000 rpm. After the addition, the stirring was done for 90 minutes at 1000 rpm.

To synthesize the Ag2HA and Ag4HA nanopowder, 0.02M AgNT was dissolved in 0.98M CNT for Ag2HA and 0.04M AgNT was dissolved in 0.96M CNT for Ag4HA. The rest procedure was followed as for synthesis of HA. The sols were aged for 24 hrs followed by their drying at 80^{o}C and then calcinations at 400^{o}C.

2.3 Coatings on substrate

The coatings were deposited by spin coating technique using parameters: spinning speed= 3500 rpm, acceleration= 10 sec and time= 10 sec. The coatings were dried at 95^{o}C for 15 minutes and then sintered at 400^{o}C for 2 hrs.
Figure. 1 gives the consolidated protocol used in this work to synthesize HA, Ag2HA and Ag4HA powders and their coatings on 316L SS.

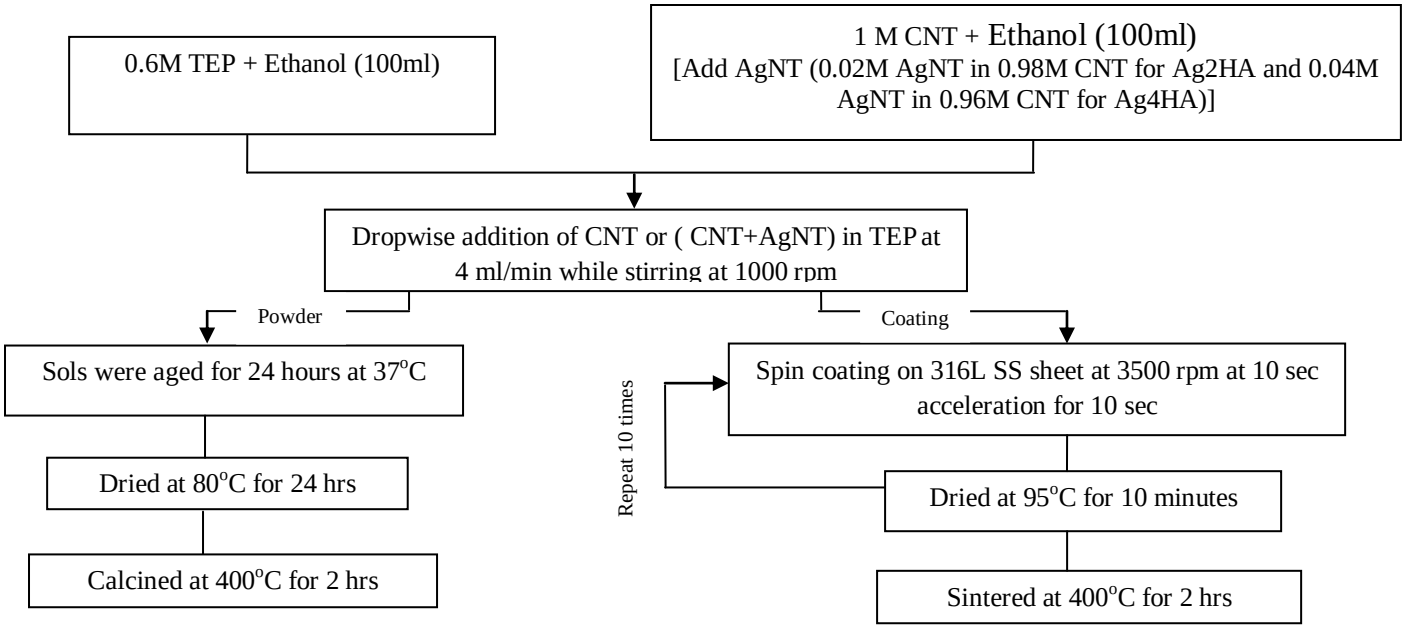

Figure 1: *Protocol for Synthesis of powder and coating of HA, Ag2HA and Ag4HA*

All Rights Reserved, @IJAREST-2016

2.4 Characterization

The effect of Ag substitution on the different functional groups was identified with Fourier Transform Infrared Spectroscopy (FTIR, Perkin Elmer, RZX, USA) in the region of 400-4000 cm^{-1}. The crystal structure and phase composition of samples was determined using an X-ray diffraction (XRD, Rigaku, Ultima IV) with Cu-K_α radiation, operating at 40kV and 40 mA. A detailed scan was done over the 2θ range of 10^o to 80^o with a step size of 0.01^o. The elemental composition was determined with X-Ray Fluorescence (XRF, Bruker, S8 Tiger, Germany). The Microstructural features and uniformity of coating was determined using Field Emission Scanning Electron Microscope (FE-SEM, Hitachi, SU8010).

The micro hardness test on coated samples was conducted using a Vicker's micro hardness tester (Huayin, HV-1000 V,) with a load of 10 gm and a dwelling time of 10 sec. The adhesion strength of the coating layer was calculated from the Vickers hardness by using the following equation:

$$Adhesion\ Strength = \left(\frac{VHN}{3}\right) 0.1^n \quad (1)$$

III. Results and Discussion

3.1 Structural Characterization by XRD, XRF and FTIR

Figure. 2 shows the FTIR spectra of HA, Ag2HA and Ag4HA samples. The peaks 3402 and 1630 cm^{-1} correspond to adsorbed water at the surface of the synthesized powders [7]. The characteristic signature HA double bands near 3572 cm^{-1} attributed to OH stretching bond and 630 cm^{-1} for OH vibrational absorption bands for all HA, Ag2HA and Ag4HA samples. Peaks 569 and 598 are attributed to O-H-O bending mode (ν_4) for HA, Ag2HA and Ag4HA samples. 1023 and 1086 cm^{-1}, 1011 and 1086 cm^{-1}, 1008 and 1086 cm^{-1} to asymmetric stretching vibration (ν_3) for HA, Ag2HA and Ag4HA. 470 is the O-H-O (ν_2) vibration and 968 to symmetric stretching vibration (ν_1) [8]. CO_3^{2-} in the spectrum shows that CO_2 is absorbed form the environment during synthesis of HA. The FTIR spectra of the different concentration of Ag2HA and Ag4HA are similar to those reported for HA. Not much significant changes in the shapes and intensities of the peaks were observed for all the samples which indicate that no structural modification of HA due to the substitution of Ag was observed [9]. FTIR results confirmed the formation of hydroxyapatite.

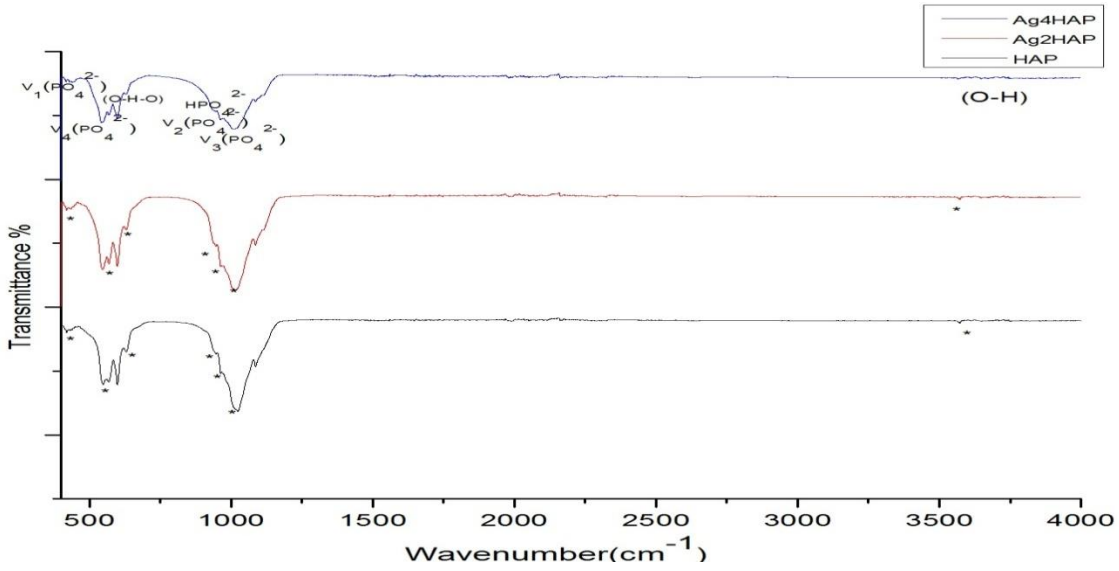

Figure 2: *FTIR results of HA, Ag2HA and Ag4HA*

Figure. 3 shows the XRD pattern of HA, Ag2HA and Ag4HA samples. The peaks (002), (300), (211) and (112) were sharp and distinct in all powders which show that HA was successfully synthesized in HA, Ag2HA and Ag4HA nanopowders. The lattice parameters of all HA, Ag2HA and Ag4HA powder were close to the HA of stoichiometric HA which indicates that the HA powder synthesized in the present work represents the stoichiometric HA [JCPDS File # 09-0432]. When the silver is substituted in HA then the diffraction peaks shifted to lower 2θ values [8],[9]. The samples with silver content exhibited a shoulder at $2\theta = 38^o$ attributable to metallic silver [12]. The percentages of HA and β-TCP

All Rights Reserved, @IJAREST-2016

phases, the crystallite size (X_s), crystallinity percent (X_C %), Ca/P ratio and lattice parameters (a & c) were calculated and given in Table 2.

As it is given in Table 2, when silver is doped in hydroxyapatite lattice parameters increases. As the ionic radius of silver (0.128 nm) is higher than the ionic radius of calcium (0.099 nm) due to which it distorts the structure and it results in increase in lattice parameters [6]. Crystallinity decreases from 96.9% HA and 67.3% Ag2HA to 54.14% Ag4HA and crystalline size decreases from 22.3 to 17.25 Å [13]. . Percentage of HA decreases from 79% HA and 78% Ag2HA to 64% Ag4HA and of β-TCP increases from 21% HA and 22% Ag2HA to 36% Ag4HA, it means when more silver is doped in HA then more β-TCP will be formed.

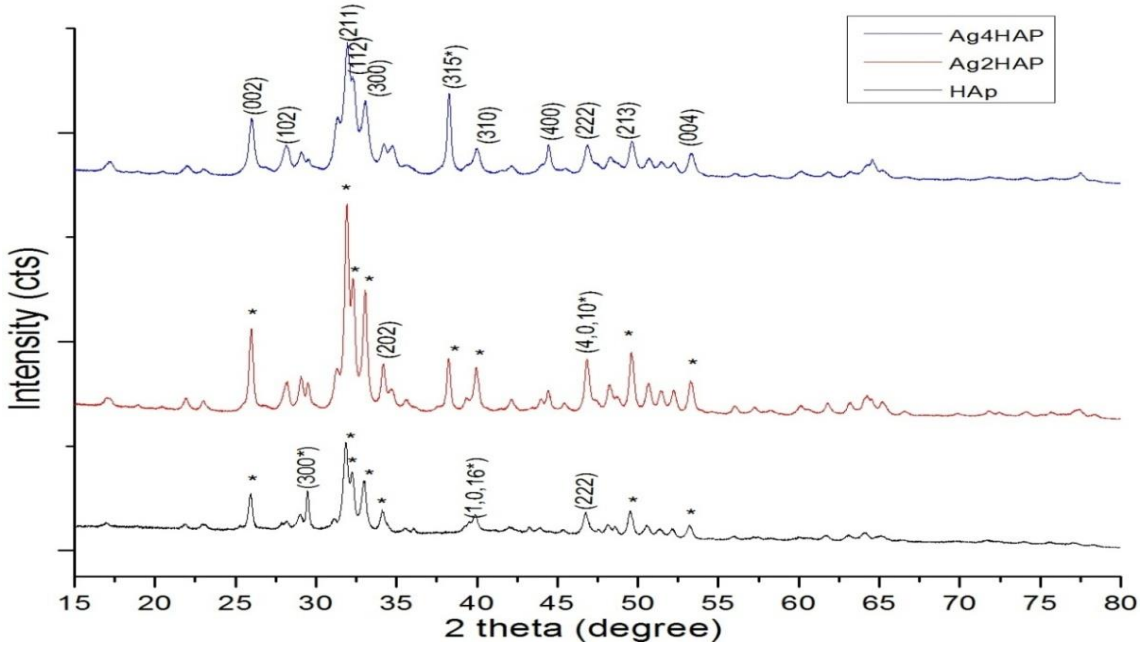

Figure 3: *XRD results of HA, Ag2HA and Ag4HA*

The crystallinity percent (X_C%) for the samples was determined by the following relation [13] and the values are shown in the Table 2.

$$\chi_c = \left(1 - \frac{V_{112/300}}{I_{300}}\right) \times 100 \quad (2)$$

Table 2: *The parameters calculated from XRD patterns*

Sample	HA (%)	β-TCP (%)	c	a	c/a	Ca/P or (Ca+Ag)/P	Crystallite size (X_s)	Crystallinity (X_c %)
HA	79	21	6.8434	9.3783	0.729	1.6156	22.3	96.9
Ag2HA	78	22	6.8558	9.3833	0.730	1.6148	18.75	67.3
Ag4HA	64	36	6.8644	9.4163	0.728	1.6141	17.25	54.14

All Rights Reserved, @IJAREST-2016

The XRF pattern of Ag2HA and Ag4HA is shown in Figure. 4. The doping of silver in hydroxyapatite nanopowder is thus confirmed from XRF results. The amount of silver in hydroxyapatite was 2.15% and 4.30% for Ag2HA and Ag4HA, respectively, which is same as the amount added during synthesis. Moreover, the results indicate the (Ca+Ag)/P ratio of powder was 1.96 and 1.82 for Ag2HA and Ag4HA, respectively, which indicates that HA formation was incomplete. The results are also supported by the presence of HPO_4^- peak in FTIR.

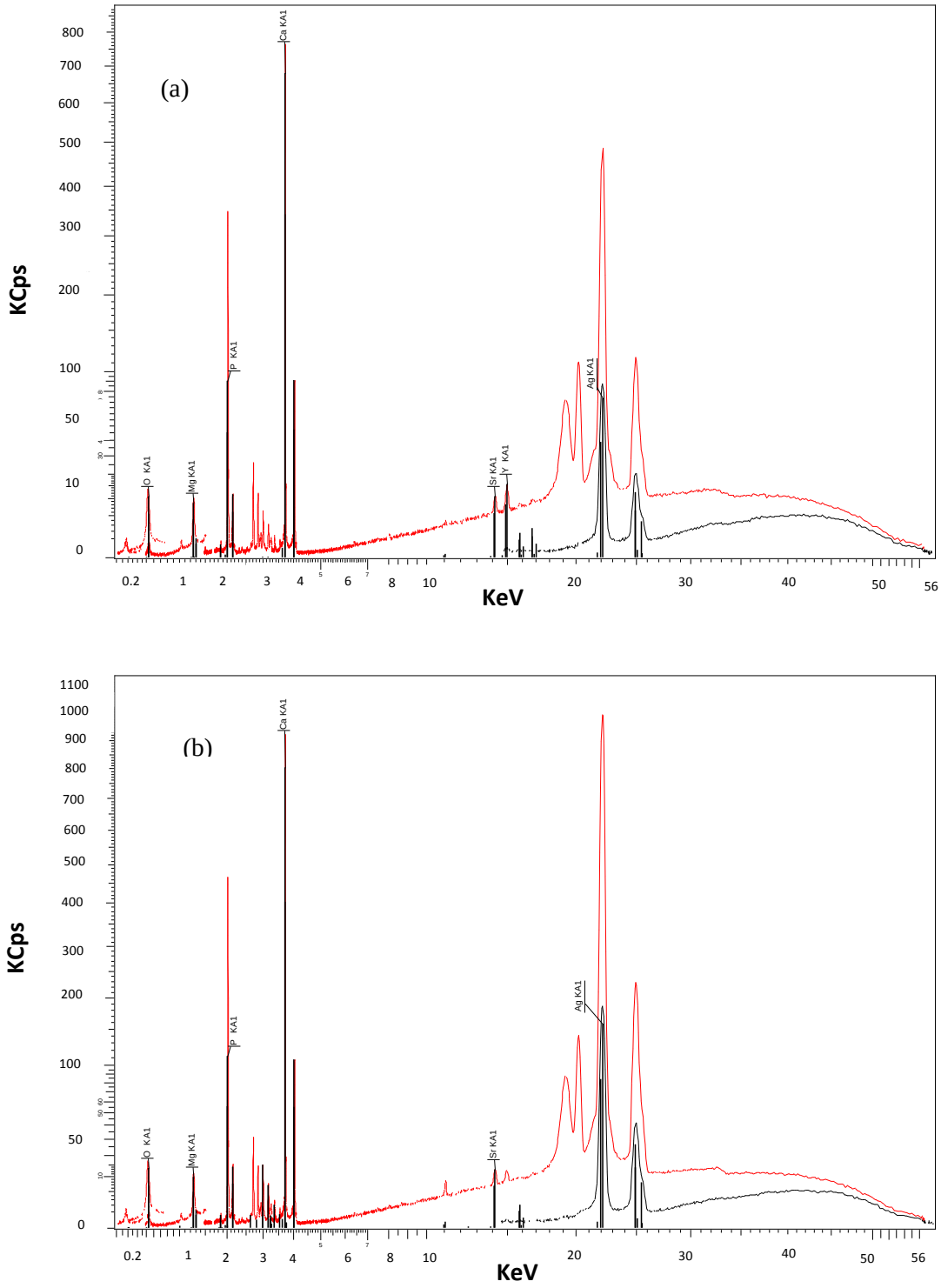

Figure 4: *XRF results of (a) Ag2HA and (b) Ag4HA*

All Rights Reserved, @IJAREST-2016

3.2 Morphological study of coated samples

The Field emission scanning electron microscopy (FE-SEM) micrographs of HA, Ag2HA and Ag4HA are shown in Figure. 5. The micrographs show that HA, Ag2HA and Ag4HA coatings were successfully deposited on 316L SS. Moreover, theses coatings were uniform but porous. Figures suggested that the substitution of Ag ions in HA has influenced the morphology of HA. The micrograph obtained for the HA is shown in Figure. 5(a),(d) which demonstrates the formation of irregular elongated and rod like shaped particles. Ag2HA coated samples composed of different spherical and irregular rod like particles and more porous than HA. Ag4HA coated samples composed of different needle and irregular particles. The bright particle which is shown in Figure. 5(b),(e) and 5(c),(f) shows the presence of silver particles and confirms that silver is present in the coating. Among all coatings, Ag4HA coating found to be dense.

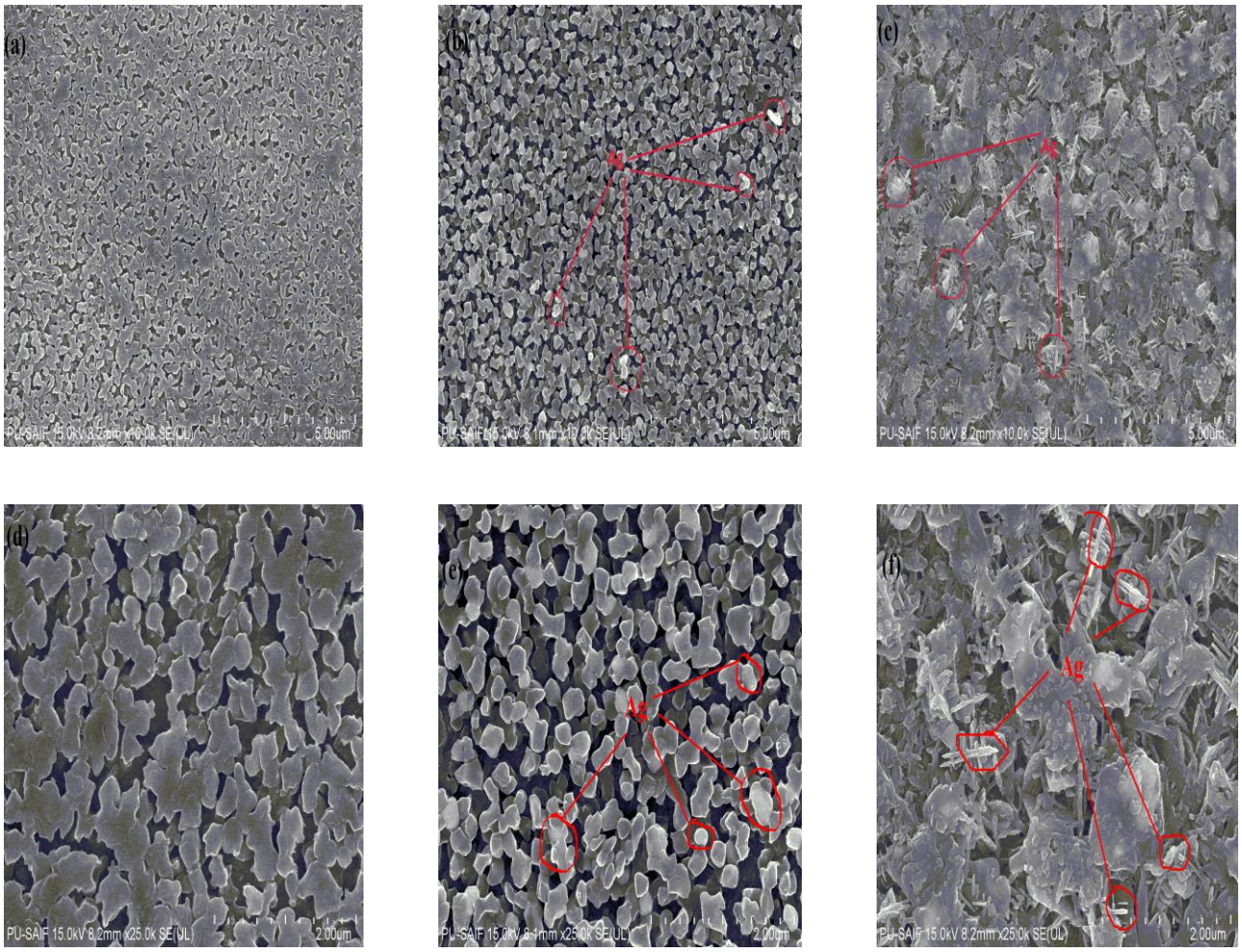

Figure 5: *FE-SEM images at 10k of (a) HA (b) Ag2HA (c) Ag4HA and at 25k of (d) HA (e) Ag2HA (f) Ag4HA*

3.3 Mechanical properties of coated samples

The vicker's micro hardness and adhesion strength of bare SS, HA, Ag2HA and Ag4HA are shown in Figure. 6. It is given in Table. 3, Ag4HA has high micro hardness and high adhesion strength.

All Rights Reserved, @IJAREST-2016

Table 3: *Vicker's micro hardness and adhesion strength of bare SS, HA, Ag2HA and Ag4HA on 316L SS coatings*

Sample	Vicker's micro hardness (VHN)	Adhesion strength
HA	118.3	39.43
Ag2HA	121.1	40.36
Ag4HA	123.6	41.20

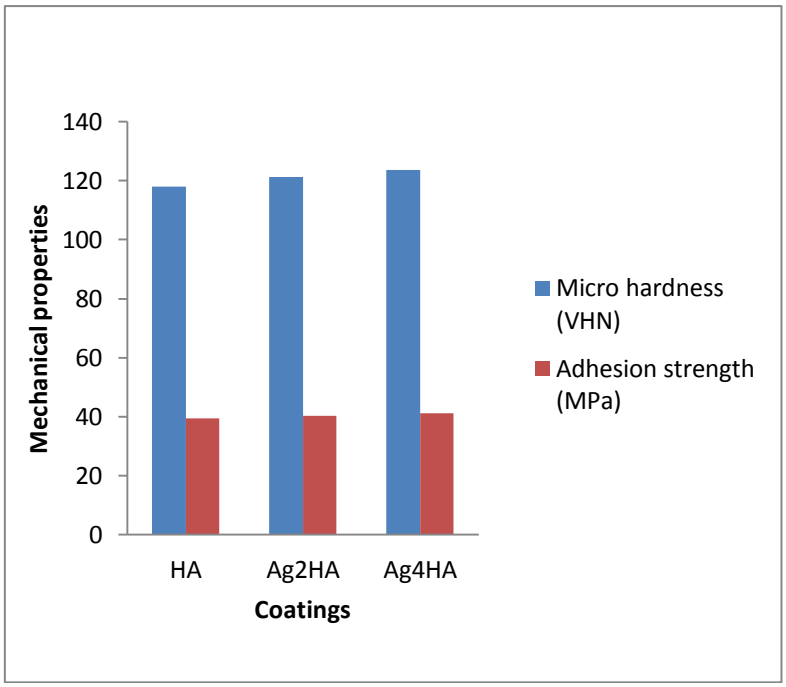

Figure 6: *Comparison of surface roughness, Vicker's micro hardness and Adhesion strength of the HA, Ag2HA and Ag4HA*

IV. CONCLUSIONS

1. Silver has been doped successfully in HA and doped amount is equal to the amount added initially during synthesis
2. HA, Ag2HA and Ag4HA coatings have been successfully and uniformly deposited on 316L SS using sol-gel spin coating technique.
3. The micro hardness of HA coatings, Ag2HA coatings and Ag4HA coatings following a decreasing order; Ag4HA > Ag2HA > HA.
4. The adhesion strength of HA coatings, Ag2HA coatings and Ag4HA coatings following a decreasing order; Ag4HA > Ag2HA > HA.

References

[1] J. Ballarre, D. Lopez, W. H. Schreiner, A. Duran, and S. M. Cere, "Protective hybrid sol-gel coatings containing bioactive particles on surgical grade stainless steel: Surface characterization," *Appl. Surf. Sci.*, vol. 253, no. 17, pp. 7260–7264, 2007.

[2] A. Mina, A. Castaño, J. C. Caicedo, H. H. Caicedo, and Y. Aguilar, "Determination of physical properties for β-TCP + chitosan biomaterial obtained on metallic 316L substrates," *Mater. Chem. Phys.*, vol. 160, pp. 296–307,

All Rights Reserved, @IJAREST-2016

2015.

[3] V. K. Balla, M. Das, S. Bose, G. D. Janaki Ram, and I. Manna, "Laser surface modification of 316 L stainless steel with bioactive hydroxyapatite," *Mater. Sci. Eng. C*, vol. 33, no. 8, pp. 4594–4598, 2013.

[4] A. Balamurugan, S. Kannan, and S. Rajeswari, "Evaluation of TiO_2 coatings obtained using the sol–gel technique on surgical grade type 316L stainless steel in simulated body fluid," *Mater. Lett.*, vol. 59, no. 24–25, pp. 3138–3143, 2005.

[5] M. Murphy, K. Ting, X. Zhang, C. Soo, and Z. Zheng, "Current Development of Silver Nanoparticle Preparation , Investigation , and Application in the Field of Medicine," *J. Nanomater.*, vol. 2015, pp. 1–12, 2015.

[6] Y. Yan, X. Zhang, Y. Huang, Q. Ding, and X. Pang, "Applied Surface Science Antibacterial and bioactivity of silver substituted hydroxyapatite / TiO_2 nanotube composite coatings on titanium," *Applied Surface Science.*, vol. 314, pp. 348–357, 2014.

[7] D. Gopi, E. Shinyjoy, and L. Kavitha, "Spectrochimica Acta Part A: Molecular and Biomolecular Spectroscopy Synthesis and spectral characterization of silver/magnesium co-substituted hydroxyapatite for biomedical applications," *Spectrochimica Acta Part A.*, vol. 127, pp. 286–291, 2014.

[8] A. Rajendran, R. C. Barik, D. Natarajan, and M. S. Kiran, "Synthesis , phase stability of hydroxyapatite–silver composite with antimicrobial activity and cytocompatability," *Ceramics International*, vol. 40, pp. 10831–10838, 2014.

[9] A. Properties and T. S. S. Kumar, "Strontium-Substituted Calcium Deficient Hydroxyapatite Nanoparticles: Synthesis , Strontium-Substituted Calcium Deficient Hydroxyapatite Nanoparticles :," *J. Am. Ceram. Soc.*, Vol. 95, no. 9, 2012.

[10] Z. Geng, Z. Cui, Z. Li, S. Zhu, Y. Liang, Y. Liu, X. Li, and X. He, "Strontium incorporation to optimize the antibacterial and biological characteristics of silver-substituted hydroxyapatite coating," *Mater Sci Eng C Mater Biol Appl,.* vol. 58, pp. 467–477, 2016.

[11] W. Chen, S. Oh, A. P. Ong, N. Oh, Y. Liu, H. S. Courtney, M. Appleford, J. L. Ong, and C. E. T. Al, "Antibacterial and osteogenic properties of silver-containing hydroxyapatite coatings produced using a sol gel process," *J Biomed Mater Res A* Vol. 82, no. 4, pp. 899-906, 2007.

[12] S. Jadalannagari and K. Deshmukh, "Antimicrobial activity of hemocompatible silver doped hydroxyapatite nanoparticles synthesized by modified sol – gel technique," *Appl Nanosci.*, Vol. 4, pp. 133–141, 2014.

[13] O. Kaygili, S. Keser, S. V Dorozhkin, and F. Yakuphanoglu, "Structural and Dielectrical Properties of Ag- and Ba-Substituted Hydroxyapatites," *J Inorg Organomet Polym.*, Vol. 24, pp. 1001–1008, 2014.

All Rights Reserved, @IJAREST-2016